Post-Print

This is the accepted version of:

A. Tamer, P. Masarati
Sensitivity of Trajectory Stability Estimated by Lyapunov Characteristic Exponents
Aerospace Science and Technology, Vol. 47, 2015, p. 501-510
doi:10.1016/j.ast.2015.10.015

Sensitivity of Trajectory Stability Estimated by Lyapunov Characteristic Exponents

Pierangelo Masarati†, Aykut Tamer
†pierangelo.masarati@polimi.it
Dipartimento di Scienze e Tecnologie Aerospaziali, Politecnico di Milano, Italy

Abstract

This work discusses the use of Lyapunov characteristic exponents for stability evaluation, and the analytical estimation of their sensitivity to parameters of the problem. The parametric sensitivity of the stability is formulated to provide a methodology for robustness analysis and design of dynamical systems with a complexity level varying from linear time invariant to nonlinear, non-autonomous. Characteristic exponents estimation and the analytical formulation of their sensitivity are based on the discrete QR decomposition method. The proposed methodology is illustrated considering the flapping of a helicopter blade, and helicopter ground resonance with one damper inoperative and with nonlinear blade dampers. Some aspects of characteristic exponents and sensitivity estimation from problems with complex conjugated modes, which are typical of mechanical and aerospace systems, are discussed.

Keywords: Stability, Lyapunov Characteristic Exponents, Analytical Sensitivity, Discrete QR Method

1. Introduction

The stability of equilibrium points $\boldsymbol{x}_0$ of nonlinear, autonomous (i.e. not explicitly dependent on time) problems $\dot{\boldsymbol{x}} = \boldsymbol{f}(\boldsymbol{x})$ can be evaluated by considering a linearization about the points themselves, according to the Hartman-Grobman theorem [1], when the real part of the eigenvalues of $\boldsymbol{f}_{/\boldsymbol{x}}$ is non zero; otherwise, the Center Manifold theorem [2] can be used. When the problem $\dot{\boldsymbol{x}} = \boldsymbol{f}(\boldsymbol{x}, t)$ is nonlinear and non-autonomous but time-periodic, of period T, the stability of periodic orbits $\boldsymbol{x}_0(t)$, such that $\boldsymbol{x}_0(t+T) = \boldsymbol{x}_0(t)\ \forall t$, can be evaluated using the Floquet-Lyapunov theory, after linearization about those orbits.

The practical, quantitative way of measuring stability depends on whether a system is autonomous and linear. Linear Time Invariant (LTI) and Linear Time Periodic (LTP) problems typically result from the linearization of nonlinear, non-autonomous problems about a steady (both LTI and LTP) or a periodic (LTP only) reference solution. They rely on eigenanalysis of special matrices and require the existence of such solutions, and the capability to identify and compute it. Obtaining a steady or periodic solution by numerical integration in time requires that solution to be stable; its computation must start from within its region of attraction. Thus, the study of the stability of the solution is actually the study of *how much stable it is*, namely of its stability margin.

A method that does not require a special reference solution (i.e. a stable point or a stable orbit) but, on the contrary, provides indications about the existence of an *attractor*, being it a point, a periodic orbit or a higher-order solution (e.g. a multidimensional torus), while computing the evolution of the system towards it, would give valuable insight into the system properties and, at the same time, provide a viable and practical means for its analysis. Lyapunov Characteristic Exponents (LCE), or in short Lyapunov Exponents, are indicators of the nature and of the stability properties of solutions of differential equations (see for example Refs. [3, 4] and references therein). They define the spectrum of the related Cauchy (initial value) problem. Lyapunov theory can be applied to nonlinear, non-autonomous systems of differential equations. The stability of trajectories in state space can be estimated while computing their evolution. The possibility to extend the approach to systems of differential-algebraic equations, as outlined for example in Refs. [5, 6, 7, 8, 9, 10], represents a promising development, in view of their use in the formulation of modern multibody dynamics.

In a dynamical system, especially when it is used for design, the rate of change of stability estimates with respect to a parameter plays a significant role if the value of that parameter is expected to change, to be modified in later design phases, or is uncertain. Such sensitivity is useful to gain insight into the dependence of stability indicators on system parameters, or can be integrated into gradient-based (or gradient-aware) optimization procedures [11] and continuation algorithms [12], or into uncertainty evaluation problems (See Ref. [13] for an example of helicopter blade aeroelastic tailoring). Sensitivity to design parameters can be estimated analytically or numerically. For nonlinear, non-autonomous problems, and thus for linear problems resulting from linearization, a change in the value of a parameter does change not only the stability properties but also the trajectory, whereas stability estimation is independent of the trajectory for linear systems. Hence, the development of analytical sensitivity estimation is preferable to finite differentiation to avoid problems related to sharp changes in sensitivity parameters, and to gain the capability to detect such topology changes of the solution and track them using continuation algorithms. The detection of a Hopf bifurcation is an example of such a topology change in which the real part of the critical characteristic exponents presents a singularity in the sensitivity when the parameter approaches a critical value [14].

The estimation of analytical sensitivity of stability parameters have been studied in the literature based on linearity and periodicity assumptions (for example, Adrianova in Ref. [3] studied the sensitivity of the spectrum of linear systems to parameter uncertainty; Shih et al. in Ref. [15] discussed parametric sensitivity of nonlinear and periodic systems). This work presents an original contribution to the practical computation of the analytical sensitivity of LCE estimates to changes in system parameters for nonlinear, non-autonomous problems. The analytical sensitivity problem is based on the Discrete QR method, which exploits the QR decomposition of the state transition matrix $\boldsymbol{Y}(t, t_0)$ of a differential problem using the tangent manifold of the so-called *fiducial trajectory*. The sensitivity of LCE estimates obtained using the discrete QR method can be practically performed in a cascaded manner:

- the LCEs are estimated using the QR decomposition of the state transition matrix from time t_0 to t, $\boldsymbol{QR} = \boldsymbol{Y}(t, t_0)$;
- the sensitivity of the LCEs is expressed as a function of the sensitivity of the diagonal elements of matrix $\boldsymbol{R}$;
- the sensitivity of matrix $\boldsymbol{R}$ is computed as a function of the sensitivity of submatrices $\boldsymbol{R}_j$ resulting from the piecewise integration of the problem from time step t_{j-1} to t_j, $\boldsymbol{Y}_j$: $\dot{\boldsymbol{Y}} = \boldsymbol{AY}$, $\boldsymbol{Y}_0 = \boldsymbol{Y}_{j-1}$;
- the sensitivity of each submatrix is computed from the sensitivity of the piecewise solutions of the problem, $\boldsymbol{Y}_{j/p}$;
- the computation of the sensitivity matrix $\boldsymbol{Y}_{j/p}$ is written in form of a self-adjoint problem, to minimize the number of time integrations regardless of the number of parameters for which sensitivity is sought.

The proposed analysis is applied to aerospace (mostly rotorcraft) related problems.

2. Spectrum of Non-Autonomous Problems and Its Sensitivity

This section recalls the definition of non-autonomous problems and of LCEs as a measure of their spectrum, numerical procedures for their estimation, and the procedure for the estimation of their sensitivity to system parameters. The derivation of the algorithm for LCEs estimate sensitivity is presented in a top-down fashion.

2.1. Non-Autonomous Problems

In engineering practice, initial value, or Cauchy, differential problems of the form

$$\dot{\boldsymbol{x}} = \boldsymbol{f}(\boldsymbol{x}, t), \qquad \boldsymbol{x}(t_0) = \boldsymbol{x}_0 \tag{1}$$

often arise. Special cases occur when the problem is linear, i.e. $\boldsymbol{f}(\boldsymbol{x}, t) = \boldsymbol{A}(t)\boldsymbol{x}(t)$, and in particular periodic, i.e. linear with $\boldsymbol{A}(t + T) = \boldsymbol{A}(t)$ for a given constant T, called the period, $\forall t$. Autonomous problems arise when $\boldsymbol{f}(\boldsymbol{x})$ does not explicitly depend on time t; a special case occurs when the problem is linear, i.e. $\boldsymbol{f}(\boldsymbol{x}) = \boldsymbol{Ax}$, with $\boldsymbol{A}$ constant, leading to a LTI problem. Stability indicators are the real part of the eigenvalues of matrix $\boldsymbol{A}$ for LTI systems, the logarithm of the real part of the eigenvalues of the monodromy matrix divided by the period for LTP problems and, as discussed in this work, LCEs for nonlinear, non-autonomous problems, a definition that includes LTI and LTP ones as special cases.

2.2. *Lyapunov Characteristic Exponents*

Given the problem of Eq. (1), with the state $\boldsymbol{x} \in \mathbb{R}^n$, the time $t \in \mathbb{R}$, and the nonlinear function $\boldsymbol{f} \in \mathbb{R}^{n+1} \to \mathbb{R}^n$, and a solution $\boldsymbol{x}(t)$ for given initial conditions $\boldsymbol{x}(t_0) = \boldsymbol{x}_0$, its Lyapunov Characteristic Exponents λ_i are defined as[1]

$$\lambda_i = \lim_{t\to\infty} \frac{1}{t} \log \|{}_i\boldsymbol{x}(t)\| \,, \tag{2}$$

where ${}_i\boldsymbol{x}(t)$ is the solution that describes the exponential evolution of the i-th axis of the ellipsoid that grows from an initially infinitesimal n-sphere according to the map $\boldsymbol{f}_{/\boldsymbol{x}}$ tangent to $\boldsymbol{f}$ along the fiducial trajectory $\boldsymbol{x}(t)$, i.e. the solution of the linear, non-autonomous problem ${}_i\dot{\boldsymbol{x}}(t) = \boldsymbol{f}_{/\boldsymbol{x}}(\boldsymbol{x}(t), t)\, {}_i\boldsymbol{x}(t)$, with ${}_i\boldsymbol{x}(t_0) = {}_i\boldsymbol{x}_0$. The definition involves the limit for $t \to \infty$; hence, in practice LCEs can only be numerically estimated for a sufficiently large value of t. In this study, unless explicitly stated, with the term "LCEs" we refer to their estimation using a large enough value of t.

LCEs represent a measure of the rate of growth of perturbed solutions. Consider infinitesimal, independent perturbations of the states with respect to a solution $\boldsymbol{x}(t)$ of Eq. (2) (the fiducial trajectory). The perturbed solution can be computed in terms of the state transition matrix $\boldsymbol{Y}(t, t_0)$, considering $\boldsymbol{A}(\boldsymbol{x}, t) = \boldsymbol{f}_{/\boldsymbol{x}}$, as the solution of the problem

$$\dot{\boldsymbol{Y}}(t, t_0) = \boldsymbol{A}(\boldsymbol{x}, t)\boldsymbol{Y}(t, t_0), \qquad \boldsymbol{Y}(t_0, t_0) = \boldsymbol{I}. \tag{3}$$

According to the Ostrogradskiĭ-Jacobi-Liouville formula [3], the determinant of $\boldsymbol{Y}(t, t_0)$ (the *Wronskian determinant* of the independent solutions that constitute $\boldsymbol{Y}(t, t_0)$) is

$$\det(\boldsymbol{Y}(t, t_0)) = \det(\boldsymbol{Y}(t_0, t_0))\, \mathrm{e}^{\int_{t_0}^{t} \mathrm{tr}(\boldsymbol{A}(\tau))\ \mathrm{d}\tau}, \tag{4}$$

where $\mathrm{tr}(\cdot)$ is the trace operator. Thus, the Wronskian never vanishes when $\boldsymbol{A}(t)$ is regular in $[t_0, t]$, since $\boldsymbol{Y}(t_0, t_0) \equiv \boldsymbol{I}$. The Wronskian geometrically represents the evolution in time of the volume of an infinitesimal portion of the state space.

The evolution of an arbitrary perturbation ${}_i\boldsymbol{x}(t_0) = {}_i\boldsymbol{x}_0$ is ${}_i\boldsymbol{x}(t) = \boldsymbol{Y}(t, t_0)\, {}_i\boldsymbol{x}_0$. As such, the contraction or expansion rate along the direction of ${}_i\boldsymbol{x}$ is estimated by considering

$$\left(\mathrm{e}^{\chi_i t}\right)^2 = \lim_{t\to\infty} \frac{{}_i\boldsymbol{x}^T {}_i\boldsymbol{x}}{{}_i\boldsymbol{x}_0{}^T {}_i\boldsymbol{x}_0} = \lim_{t\to\infty} \frac{{}_i\boldsymbol{x}_0{}^T \boldsymbol{Y}^T \boldsymbol{Y}\, {}_i\boldsymbol{x}_0}{{}_i\boldsymbol{x}_0{}^T {}_i\boldsymbol{x}_0}. \tag{5}$$

Consider now the singular value decomposition (SVD) of $\boldsymbol{Y}(t, t_0)$,

$$\boldsymbol{U}\boldsymbol{\Sigma}\boldsymbol{V}^T = \boldsymbol{Y}(t, t_0), \tag{6}$$

[1] Actually, Eq. (2) should be

$$\lambda_i = \lim_{t\to\infty} \frac{1}{t} \log \frac{\|{}_i\boldsymbol{x}(t)\|}{\|{}_i\boldsymbol{x}(t_0)\|};$$

however, one can easily prove that for any finite constant c the LCE of $cf(x, t)$ is equal to that of $f(x, t)$.

where $\boldsymbol{U} = \boldsymbol{U}(t)$ and $\boldsymbol{V} = \boldsymbol{V}(t)$ are orthogonal matrices. The singular values σ_i, namely the diagonal elements of $\boldsymbol{\Sigma} = \boldsymbol{\Sigma}(t)$, which are strictly greater than zero as a consequence of the above mentioned Ostrogradskiĭ-Jacobi-Liouville formula[2], express the growth of the perturbed solution along orthogonal directions $\boldsymbol{U}(t)\,_i\boldsymbol{x}_0$ in the state space.

In the approximation of LCEs, one important issue is that of continuity with respect to perturbations. This aspect can be particularly critical when sensitivity is addressed. It is known that the property of integral separation is a necessary and sufficient condition for the computability of distinct LCEs [16]. This result has been extended to the case of multiple LCEs, i.e. sets of LCEs which converge to same value [17].

So-called continuous formulas for the estimation of the LCEs can be derived from the definition based on the SVD, as well as on the QR decomposition (see for example [18]). Such formulas originally suffered from the numerical difficulty of dealing with matrices whose coefficients either rapidly converge to zero (exponential stability) or diverge (instability), although in recent times they have seen extensive development [19, 20, 21, 22]. For this reason, different approaches have been formulated; the so-called discrete QR method, based on the incremental use of the QR decomposition of the state transition matrix for each time step, is discussed in the next section.

2.3. The Discrete QR Method

The definition of Eq. (2) is not practical, because the determinant of the state transition matrix usually either contracts to zero or expands to infinity, depending on the (lack of) stability of the solution, thus either over- or underflowing. The practical computation of LCEs requires one to exploit re-orthogonalization of local directions of evolution of the solution, as proposed in the seminal work of Benettin *et al.* [4], which first showed that the computation of LCEs could be practically and effectively achieved. Numerical methods have been devised for this purpose. A most popular one is the so-called Discrete QR method, which is based on incrementally updating the LCE estimates with the contribution of the diagonal elements of the matrix $\boldsymbol{R}$ resulting from the QR decomposition of the state transition matrix between two consecutive time steps.

The state transition matrix $\boldsymbol{Y}(t, t_0)$ from an arbitrary initial time t_0 to an arbitrary time t is the solution of the problem $\dot{\boldsymbol{Y}} = \boldsymbol{f}_{/\boldsymbol{x}}(\boldsymbol{x}(t), t)\boldsymbol{Y}$ with $\boldsymbol{Y}(t_0, t_0) = \boldsymbol{I}$. Its QR decomposition yields $\boldsymbol{Y}(t, t_0) = \boldsymbol{Q}(t)\boldsymbol{R}(t, t_0) = \boldsymbol{Q}(t)\boldsymbol{R}(t)$, where the initial time t_0 has been omitted from matrix $\boldsymbol{R}$ for clarity. The state transition matrix from time t_0 to time t_j, $\boldsymbol{Y}(t_j, t_0)$, can be split as $\boldsymbol{Y}(t_j, t_0) = \boldsymbol{Y}(t_j, t_{j-1})\boldsymbol{Y}(t_{j-1}, t_0)$. Consider now the QR decomposition $\boldsymbol{Y}(t_{j-1}, t_0) = \boldsymbol{Q}(t_{j-1})\boldsymbol{R}(t_{j-1})$ which, combined with that of the complete state transition matrix, yields

$$\boldsymbol{Q}(t_j)\boldsymbol{R}(t_j) = \boldsymbol{Y}(t_j, t_{j-1})\boldsymbol{Q}(t_{j-1})\boldsymbol{R}(t_{j-1}). \tag{7}$$

[2]After choosing $\boldsymbol{Y}(t_0, t_0) = \boldsymbol{I}$, its determinant is 1; the integral of matrix $\boldsymbol{A}(t)$ is finite, and thus its exponential is a strictly positive number.

Consider now the QR decomposition of matrix $\boldsymbol{Y}(t_j, t_{j-1})\boldsymbol{Q}(t_{j-1}) = \boldsymbol{Q}_j\boldsymbol{R}_j$, which, replaced in Eq. (7), yields $\boldsymbol{Q}(t_j)\boldsymbol{R}(t_j) = \boldsymbol{Q}_j\boldsymbol{R}_j\boldsymbol{R}(t_{j-1})$. Clearly, $\boldsymbol{Q}_j = \boldsymbol{Q}(t_j)$ and $\boldsymbol{R}(t_j) = \boldsymbol{R}_j\boldsymbol{R}(t_{j-1})$. The LCEs are then estimated from $\boldsymbol{R}(t_j)$ as

$$\lambda_i = \lim_{j\to\infty} \frac{1}{t_j} \log r_{ii}(t_j), \tag{8}$$

where $r_{ii}(t_j)$ are the diagonal elements of matrix $\boldsymbol{R}(t_j)$.

Since the product of two upper triangular matrices $\boldsymbol{C} = \boldsymbol{AB}$ is also an upper triangular matrix, whose diagonal elements are $c_{ii} = a_{ii}b_{ii}$, the logarithm of c_{ii} can be incrementally computed as $\log(a_{ii}b_{ii}) = \log(a_{ii}) + \log(b_{ii})$, which helps prevent overflow/underflow in numerical computations. Furthermore,

$$r_{ii}(t_j) = \Pi_{k=0}^{j} r_{(j-k)_{ii}}, \tag{9}$$

where $r_{(j-k)_{ii}}$ stands for the ith diagonal element of matrix $\boldsymbol{R}_{j-k}$ that results from the incremental QR decomposition at step $j-k$; thus

$$\log\left(r_{ii}(t_j)\right) = \sum_{k=0}^{j} \log(r_{k_{ii}}), \tag{10}$$

which leads to

$$\lambda_i = \lim_{j\to\infty} \frac{1}{t_j} \sum_{k=0}^{j} \log(r_{k_{ii}}). \tag{11}$$

2.4. Sensitivity of Lyapunov Exponents Estimates

Consider a set of bounded parameters $\boldsymbol{p} \in \mathcal{P}$, and assume that the problem $\dot{\boldsymbol{x}} = \boldsymbol{f}(\boldsymbol{x}, t, \boldsymbol{p})$ depends on parameters $\boldsymbol{p}$. The sensitivity of the LCEs with respect to a generic parameter $p \subset \boldsymbol{p}$, using the form of Eq. (11), can be expressed as

$$\lambda_{i/p} = \lim_{j\to\infty} \frac{1}{t_j} \sum_{k=1}^{j} \frac{r_{k_{ii}/p}}{r_{k_{ii}}}. \tag{12}$$

In this case, only the sensitivity of $\boldsymbol{R}_j$ is needed, which is obtained in the next section by computing the sensitivity of the QR decomposition.

2.5. Sensitivity of QR Decomposition

The sensitivity of the QR decomposition can be obtained along the lines of the state transition matrix QR decomposition differentiation that is used to formulate the continuous QR method for LCE estimation (see for example [4, 23]).

Consider the QR decomposition of an arbitrary matrix $\boldsymbol{M} \in \mathbb{R}^{n\times n}$:

$$\boldsymbol{M} = \boldsymbol{QR} \tag{13}$$

with $\boldsymbol{Q}^T\boldsymbol{Q} = \boldsymbol{I}$, and $\boldsymbol{R}$ upper triangular, with positive diagonal elements. Consider the derivative of $\boldsymbol{M}$ with respect to a scalar parameter p,

$$\boldsymbol{M}_{/p} = \boldsymbol{Q}_{/p}\boldsymbol{R} + \boldsymbol{Q}\boldsymbol{R}_{/p}, \tag{14}$$

and the corresponding derivative of the orthogonality condition $\boldsymbol{Q}^T\boldsymbol{Q} = \boldsymbol{I}$,

$$\left(\boldsymbol{Q}^T\right)_{/p}\boldsymbol{Q} + \boldsymbol{Q}^T\boldsymbol{Q}_{/p} = \boldsymbol{0}, \tag{15}$$

i.e.

$$\left(\boldsymbol{Q}^T\boldsymbol{Q}_{/p}\right)^T + \boldsymbol{Q}^T\boldsymbol{Q}_{/p} = \boldsymbol{0}. \tag{16}$$

The latter condition states that $\boldsymbol{Q}^T\boldsymbol{Q}_{/p}$ must be skew-symmetric; thus, only $n(n-1)/2$ coefficients are independent (for example, those in the strictly lower triangular portion, i.e. the lower triangular part, excluding the diagonal).

Finally, premultiply $\boldsymbol{M}_{/p}$ by $\boldsymbol{Q}^T$:

$$\boldsymbol{R}_{/p} = \boldsymbol{Q}^T\boldsymbol{M}_{/p} - \boldsymbol{Q}^T\boldsymbol{Q}_{/p}\boldsymbol{R} \tag{17}$$

Since matrix $\boldsymbol{R}_{/p}$ is upper triangular, after defining operator $\mathrm{triu}(\cdot)$, which extracts the upper triangular part of the argument, and operator $\mathrm{stril}(\cdot)$, which extracts the strictly lower triangular part of the argument, the whole problem can be re-cast in the form:

$$\begin{aligned} &\text{compute} && \boldsymbol{W} = \boldsymbol{Q}^T\boldsymbol{Q}_{/p} && \text{(18a)} \\ &\text{such that} && \mathrm{stril}\left(\boldsymbol{Q}^T\boldsymbol{M}_{/p} - \boldsymbol{W}\boldsymbol{R}\right) = \mathrm{stril}\left(\boldsymbol{0}\right) && \text{(18b)} \\ &\text{subjected to} && \boldsymbol{W}^T + \boldsymbol{W} = \boldsymbol{0} && \text{(18c)} \end{aligned}$$

$$\begin{aligned} &\text{compute} && \boldsymbol{R}_{/p} && \text{(18d)} \\ &\text{such that} && \mathrm{triu}\left(\boldsymbol{R}_{/p}\right) = \mathrm{triu}\left(\boldsymbol{Q}^T\boldsymbol{M}_{/p} - \boldsymbol{W}\boldsymbol{R}\right) && \text{(18e)} \\ &\text{and} && \mathrm{stril}\left(\boldsymbol{R}_{/p}\right) = \mathrm{stril}\left(\boldsymbol{0}\right). && \text{(18f)} \end{aligned}$$

The last statement is redundant since $\boldsymbol{W}$ computed according to Eqs. (18a–c) already yields $\boldsymbol{R}_{/p}$ with the strictly lower triangular part set to zero.

It is worth noticing that, since $\boldsymbol{R}$ is upper triangular, $\boldsymbol{W}$ is computed as

$$\boldsymbol{W}_L = \mathrm{stril}\left(\boldsymbol{Q}^T\boldsymbol{M}_{/p}\boldsymbol{R}^{-1}\right) \qquad \boldsymbol{W} = \boldsymbol{W}_L - \boldsymbol{W}_L^T \tag{19}$$

where $\boldsymbol{R}^{-1}$ does not require any factorization, but only back-substitution. In fact, after setting $\boldsymbol{B} = \boldsymbol{Q}^T\boldsymbol{M}_{/p}$, the generic coefficient of $\mathrm{stril}(\boldsymbol{W})$ is

$$w_{ij} = \frac{1}{r_{jj}}\left(b_{ij} - \sum_{k=1}^{j-1} w_{ik}r_{kj}\right) \qquad j = 1, n-1 \qquad i = j+1, n. \tag{20}$$

Then

$$\boldsymbol{Q}_{/p} = \boldsymbol{Q}\boldsymbol{W}. \tag{21}$$

2.6. Sensitivity of Lyapunov Exponents Estimated by the Discrete QR Method

The discrete QR method requires the decomposition of $\boldsymbol{Y}_j\boldsymbol{Q}_{j-1}$; thus, the sensitivity of $\boldsymbol{Y}_j\boldsymbol{Q}_{j-1} = \boldsymbol{Q}_j\boldsymbol{R}_j$ is actually required, i.e.

$$\boldsymbol{Q}_{j/p}\boldsymbol{R}_j + \boldsymbol{Q}_j\boldsymbol{R}_{j/p} = \boldsymbol{Y}_{j/p}\boldsymbol{Q}_{j-1} + \boldsymbol{Y}_j\boldsymbol{Q}_{(j-1)/p}, \tag{22}$$

where $\boldsymbol{Q}_{j-1}$ and $\boldsymbol{Q}_{(j-1)/p}$ are available from the previous step.

First of all, Eq. (22) is premultiplied by $\boldsymbol{Q}_j^T$ to obtain

$$\boldsymbol{Q}_j^T\boldsymbol{Q}_{j/p}\boldsymbol{R}_j + \boldsymbol{R}_{j/p} = \boldsymbol{Q}_j^T\boldsymbol{Y}_{j/p}\boldsymbol{Q}_{j-1} + \boldsymbol{Q}_j^T\boldsymbol{Y}_j\boldsymbol{Q}_{(j-1)/p}. \tag{23}$$

Then the strictly lower triangular part of the equation is evaluated to compute $\boldsymbol{W}_L$,

$$\begin{aligned}\boldsymbol{W}_L &= \operatorname{stril}\left(\left(\boldsymbol{Q}_j^T\boldsymbol{Y}_{j/p}\boldsymbol{Q}_{j-1} + \boldsymbol{Q}_j^T\boldsymbol{Y}_j\boldsymbol{Q}_{(j-1)/p}\right)\boldsymbol{R}_j^{-1}\right)\\ &= \operatorname{stril}\left(\left(\boldsymbol{Q}_j^T\boldsymbol{Y}_{j/p}\boldsymbol{Q}_{j-1} + \boldsymbol{R}_j\boldsymbol{W}_{j-1}\right)\boldsymbol{R}_j^{-1}\right),\end{aligned} \tag{24}$$

the strictly lower triangular part of $\boldsymbol{W}_j = \boldsymbol{Q}_j^T\boldsymbol{Q}_{j/p} = \boldsymbol{W}_L - \boldsymbol{W}_L^T$. See Eq. (20) for details about the computation of $\boldsymbol{W}_L$.

Finally, the upper triangular part of Eq. (23) is evaluated to obtain $\boldsymbol{R}_{j/p}$,

$$\begin{aligned}\boldsymbol{R}_{j/p} &= \boldsymbol{Q}_j^T\left(\boldsymbol{Y}_{j/p}\boldsymbol{Q}_{j-1} + \boldsymbol{Y}_j\boldsymbol{Q}_{(j-1)/p}\right) - \boldsymbol{W}_j\boldsymbol{R}_j\\ &= \boldsymbol{Q}_j^T\boldsymbol{Y}_{j/p}\boldsymbol{Q}_{j-1} + \boldsymbol{R}_j\boldsymbol{W}_{j-1} - \boldsymbol{W}_j\boldsymbol{R}_j\end{aligned} \tag{25}$$

The sensitivity of $\boldsymbol{Y}_j$, i.e. the state transition matrix from t_{j-1} to t_j, is needed.

2.7. Sensitivity of the State Transition Matrix

The sensitivity of $\boldsymbol{Y}$ at time t_j, namely $\boldsymbol{Y}_{/p}(t_j)$, is needed to compute the sensitivity of the LCEs. In principle, this is obtained by integrating the sensitivity of the problem $\dot{\boldsymbol{Y}} = \boldsymbol{A}\boldsymbol{Y}$. Then

$$\begin{aligned}\dot{\boldsymbol{Y}}_{/p} &= \boldsymbol{A}\boldsymbol{Y}_{/p} + \left(\boldsymbol{A}_{/\boldsymbol{x}}\boldsymbol{x}_{/p} + \boldsymbol{A}_{/p}\right)\boldsymbol{Y}\\ &= \boldsymbol{A}\boldsymbol{Y}_{/p} + \frac{\mathrm{d}\boldsymbol{A}}{\mathrm{d}p}\boldsymbol{Y},\end{aligned} \tag{26}$$

i.e. a problem with the same matrix $\boldsymbol{A}$ of the original one, forced by a term $(\mathrm{d}\boldsymbol{A}/\mathrm{d}p)\boldsymbol{Y}$ that depends on the reference solution, as also noted in Ref. [15] in the context of parameter sensitivity of nonlinear periodic problems. The total derivative of the generic element of matrix $\boldsymbol{A}$ with respect to the parameter is

$$\frac{\mathrm{d}a_{ij}}{\mathrm{d}p} = \frac{\partial^2\boldsymbol{f}_i}{\partial\boldsymbol{x}_j\partial\boldsymbol{x}_k}\frac{\partial\boldsymbol{x}_k}{\partial p} + \frac{\partial^2\boldsymbol{f}_i}{\partial\boldsymbol{x}_j\partial p}. \tag{27}$$

The terms $\partial^2 \boldsymbol{f}_i/\partial \boldsymbol{x}_j \partial \boldsymbol{x}_k$ are the elements of the second-order derivative of function $\boldsymbol{f}$ with respect to the state $\boldsymbol{x}$. It vanishes for linear problems. The sensitivity of the state to the parameter p is obtained by perturbing the problem $\dot{\boldsymbol{x}} = \boldsymbol{f}(\boldsymbol{x}, t)$,

$$\dot{\boldsymbol{x}}_{/p} = \boldsymbol{f}_{/x}\boldsymbol{x}_{/p} + \boldsymbol{f}_{/p}, \tag{28}$$

and integrating it in time accordingly. A similar problem needs to be solved for each parameter.

The sensitivity of the state transition matrix $\boldsymbol{Y}_{/p}(t, t_j)$ can be calculated using the integration method that is applied to compute the state transition matrix itself. For example, if Hsu's method [24] is used to compute the state transition matrix of a Linear Time Variant (LTV) problem, the state transition matrix is readily obtained as

$$\boldsymbol{Y}(t, t_j) \approx \mathrm{e}^{\hat{\boldsymbol{A}}(t-t_j)}\boldsymbol{Y}(t_j, t_j), \tag{29}$$

where $\hat{\boldsymbol{A}}$ is a suitable average of matrix $\boldsymbol{A}$ in the neighborhood of t_j [24]; the matrix exponential may be approximated (e.g. truncated when computed as a matrix power series) to improve the computational efficiency of the method. In this case, the sensitivity of the state transition matrix can be approximated as

$$\begin{aligned}\boldsymbol{Y}_{/p}(t, t_j) &\approx \hat{\boldsymbol{A}}_{/p}(t - t_j)\mathrm{e}^{\hat{\boldsymbol{A}}(t-t_j)}\boldsymbol{Y}(t_j, t_j) \\ &= \hat{\boldsymbol{A}}_{/p}(t - t_j)\boldsymbol{Y}(t, t_j).\end{aligned} \tag{30}$$

Care must be taken in the computation of the sensitivity matrix $\boldsymbol{Y}_{/p}(t, t_j)$, as differentiation is an ill-posed problem.

2.8. Summary

In summary, the steps required for LCE estimation are:

- increment the fiducial trajectory $\boldsymbol{x}(t)$ from t_{j-1} to t_j, Eq. (1);
- compute the state transition matrix increment $\boldsymbol{Y}_j$, Eq. (3);
- compute the QR decomposition increment $\boldsymbol{Q}_j\boldsymbol{R}_j = \boldsymbol{Y}_j\boldsymbol{Q}_{j-1}$;
- update the LCE estimates using the diagonal elements of $\boldsymbol{R}_j$, Eq. (11).

The steps required for LCE sensitivity estimation are:

- if the problem is nonlinear, increment the sensitivity of the fiducial trajectory, $\boldsymbol{x}_{/p}(t)$, Eq. (28);
- compute the sensitivity of the state transition matrix increment $\boldsymbol{Y}_{j/p}$, Eq. (26);
- compute the sensitivity of the QR decomposition, $\boldsymbol{Q}_{j/p}$ and $\boldsymbol{R}_{j/p}$, Eqs. (18);

- update the LCE sensitivity estimation using the diagonal elements of $\boldsymbol{R}_{j/p}$, Eq. (12).

The computation of the fiducial trajectory, the estimation of the LCEs, and the estimation of their sensitivity can be computed sequentially, or incrementally at each time step. In the latter case, the computation can be stopped when LCE sensitivity estimation converges as desired.

3. Numerical Examples

3.1. Helicopter Blade Flapping

Rigid blade flapping can be modeled as a second order single degree of freedom LTP problem (from Ref. [25]) under simplifying assumptions. Since the purpose of this example is to address the sensitivity estimation of the stability properties of LTP systems, instead of using a more realistic but complex helicopter blade dynamics model, only periodicity is retained; the model is oversimplified by linearizing the dynamics, using quasi-static aerodynamics and neglecting reverse flow conditions. The dots represent differentiation with respect to the azimuth angle t (in this context it represents non-dimensional time). The equation of motion can be written as

$$\begin{aligned} &\ddot{\beta} + \frac{\gamma}{8}\left(1 + \frac{4}{3}\mu\sin(t)\right)\dot{\beta} + \\ &\qquad \left(\nu_\beta^2 + \frac{\gamma}{8}\left(\frac{4}{3}\mu\cos(t) + \mu^2\sin(2t)\right)\right)\beta = 0 \end{aligned} \tag{31}$$

that represents the flapping of a rigid helicopter blade, where β is the blade flap angle, γ is the Lock number (the non-dimensional ratio between aerodynamic and inertial flapping loads, which is roughly proportional to the damping factor), μ is the advance ratio (the ratio between the helicopter forward velocity and the blade tip velocity in hover, which weighs the periodic part of the coefficients) and ν_β is the non-dimensional flapping frequency. In order to demonstrate the trend of LCE estimates with respect to a parameter, the advance ratio μ is chosen.

The non-trivial trajectories can be obtained starting from arbitrary initial conditions; if $\beta(t) = 0$ is asymptotically stable, the solution converges to it. Since this problem is linear and homogeneous, $\beta(t) = 0$ is the unique equilibrium point and stability does not depend on the initial conditions.

The problem is rewritten in first order form and integrated to compute the state transition matrix at each time step. LCEs and their sensitivity are estimated according to the proposed approach. The expected fiducial trajectory is readily obtained within a few periods when it is asymptotically stable. The evolution of LCE estimates associated with complex conjugated eigenvalues ($\mu = 0.15$) is shown in Fig. 1a; a zoom is shown in Fig. 1b. Owing to periodicity, the mean value of two LCEs associated with complex conjugated eigenvalues shows a decaying oscillatory behavior with the period of the system, $T = 2\pi$. The decay is caused by division by t, according to Eq. (2).

In order to have an accurate estimate of the LCEs, integration needs to be performed for a large enough non-dimensional time, to let the oscillations vanish. It is observed that in those cases, considering the average of LCE estimates that appear to converge to the same value gives a much better estimation and allows earlier truncation of the analysis. The numerical examples reported in the following make use of this technique to improve the estimation of LCEs. More robust approaches for the detection of LCEs with multiplicity greater than one are being formulated by the authors.

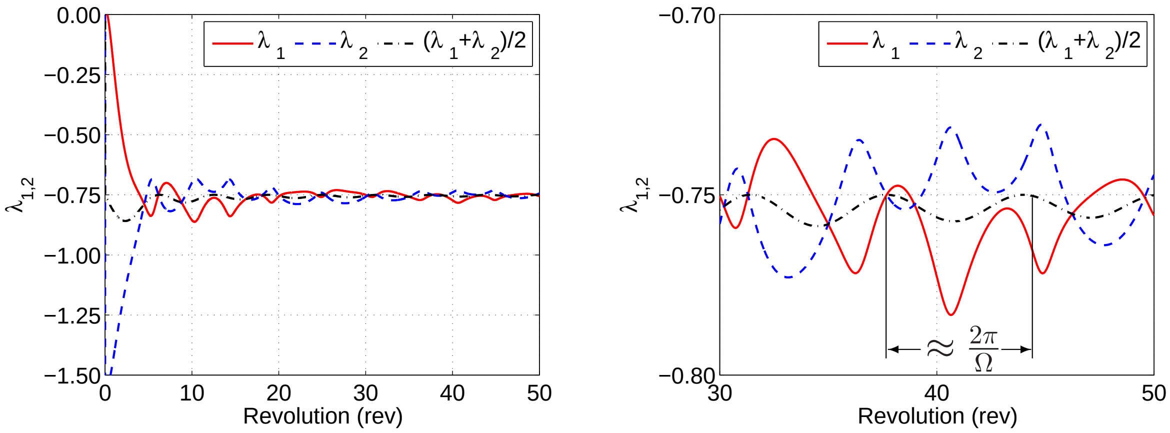

(a) Time Evolution of LCEs

(b) Zoomed after convergence

Figure 1: Blade flapping: time evolution of LCE estimates and zoomed plot after convergence, $\mu = 0.15$

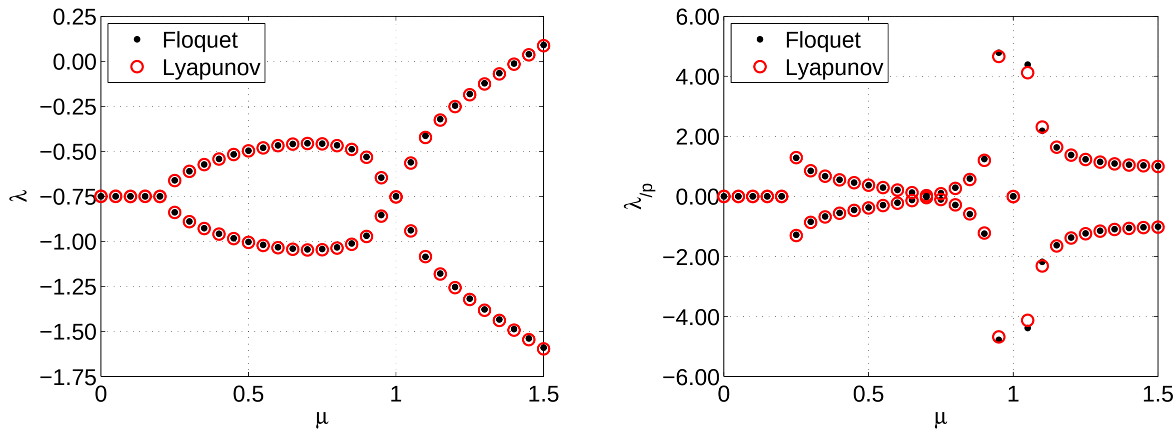

(a) LCEs

(b) Sensitivity of LCEs

Figure 2: Blade flapping: estimates of LCEs and their sensitivity with respect to advance ratio μ.

The LCEs and their sensitivity estimates are compared in Fig. 2a and Fig. 2b respectively with the corresponding sensitivity values obtained using the Floquet-Lyapunov theory according to the approach presented in [26], for a range of advance ratio $0 \leq \mu \leq 1.5$. The results are in good agreement; only where strong gradients occur the results differ slightly, probably because the LCE estimates were not sufficiently close to convergence.

3.2. Helicopter Ground Resonance with Non-Linear Lead-Lag Dampers

Ground Resonance is a mechanical instability caused by the interaction between the in-plane degrees of freedom of a helicopter rotor and the motion of the airframe (see for example [27], or the seminal work by Coleman and Feingold, [28]). The combination of the in-plane motion of the blades causes an overall in-plane motion of the rotor center of mass which couples with the dynamics of the airframe and undercarriage system. For this reason, the damping of the in-plane motion of the blades is essential in articulated and soft-inplane rotors; it is usually provided by lead-lag dampers.

Hammond's model of a four-blade rotor [29] has been extensively used due to its simplicity; as such, it is chosen as the helicopter ground resonance model in this study. The equations of motion in the rotating reference frame can be written as

$$\boldsymbol{M}_r(\psi)\ddot{\boldsymbol{q}}_r + \boldsymbol{C}_r(\psi)\dot{\boldsymbol{q}}_r + \boldsymbol{K}_r(\psi)\boldsymbol{q}_r = \boldsymbol{0} \tag{32}$$

where $\boldsymbol{q}_r$ is the degrees of freedom vector, and $\boldsymbol{M}_r$, $\boldsymbol{C}_r$, and $\boldsymbol{K}_r$ are the azimuth-dependent mass, damping and stiffness matrices in the rotating frame, with periodic terms as given in the original work [29]. Hammond's model considers four blade degrees of freedom (ζ_i, $i \in [1, N]$ being the blade index, with $N = 4$) and two hub in-plane degrees of freedom, x being longitudinal (rotor head displacement due to pitch) and y being lateral (rotor head displacement due to roll). Therefore,

$$\boldsymbol{q}_r = [\zeta_1 \;\; \zeta_2 \;\; \zeta_3 \;\; \zeta_4 \;\; x \;\; y]^T; \tag{33}$$

$\psi_i = \psi + i2\pi/N$ is the azimuth angle of the corresponding blade with blade index i; ψ is the reference azimuth angle. The parameter values are reported in Ref. [29].

The degrees of freedom vector and the matrices can be expressed in the non-rotating frame using the transformation matrix $\boldsymbol{T}_0$, its first time derivative $\boldsymbol{T}_1$ and second time derivative $\boldsymbol{T}_2$, normalized with the angular speed of the rotor, Ω, as described in Ref. [30]. Then, the degrees of freedom vector in the non-rotating frame is

$$\boldsymbol{q}_{nr} = \boldsymbol{T}_0^{-1}\boldsymbol{q}_r = [\zeta_0 \;\; \zeta_{1c} \;\; \zeta_{1s} \;\; \zeta_{N/2} \;\; x \;\; y]^T; \tag{34}$$

$\boldsymbol{q}_{nr}$ includes the collective, ζ_0, cyclic, ζ_{1c} and ζ_{1s}, and reactionless, $\zeta_{N/2}$ blade lead-lag coordinates, and the two hub displacement coordinates x and y, as in $\boldsymbol{q}_r$. The equation of motion in the non-rotating frame can be written as

$$\boldsymbol{M}_{nr}\ddot{\boldsymbol{q}}_{nr} + \boldsymbol{C}_{nr}\dot{\boldsymbol{q}}_{nr} + \boldsymbol{K}_{nr}\boldsymbol{q}_{nr} = \boldsymbol{0} \tag{35}$$

Table 1: Saturated hydraulic damper parameters.

$\bar{\chi}$	1.2203×10^6	$\mathrm{N\,m\,s^2\,rad^{-2}}$
$\dot{\zeta}_L$	1.0	$\mathrm{deg\,s^{-1}}$

with the corresponding non-rotating mass, $\boldsymbol{M}_{nr}$, damping, $\boldsymbol{C}_{nr}$, and stiffness, $\boldsymbol{K}_{nr}$, matrices, which are transformed from the rotating-frame matrices $\boldsymbol{M}_r$, $\boldsymbol{C}_r$ and $\boldsymbol{K}_r$ as

$$\boldsymbol{M}_{nr} = \boldsymbol{T}_1^{-1}\boldsymbol{M}_r\boldsymbol{T}_1 \tag{36}$$

$$\boldsymbol{C}_{nr} = \boldsymbol{T}_1^{-1}(2\Omega\boldsymbol{M}_r\boldsymbol{T}_2 + \boldsymbol{C}_r\boldsymbol{T}_1) \tag{37}$$

$$\boldsymbol{K}_{nr} = \boldsymbol{T}_1^{-1}(\Omega^2\boldsymbol{M}_r\boldsymbol{T}_3 + \Omega\boldsymbol{C}_r\boldsymbol{T}_2 + \boldsymbol{K}_r\boldsymbol{T}_1) \tag{38}$$

These matrices are no longer azimuth-dependent when the rotor is isotropic.

Although linearized and time-averaged models are commonly used in practice, the dynamics of helicopters is generally described by nonlinear, time-dependent equations [31]. Among nonlinear phenomena, limit cycle oscillations (LCO) are defined as isolated closed trajectories of nonlinear dynamical systems. When an LCO develops, the system oscillates in a self-sustained manner without the need of an external input [32]. Clearly, the occurrence of LCOs can affect structural life, flight safety and ride comfort of a rotorcraft; their occurrence can only be detected considering the nonlinearity of the problem.

A distinctive advantage of LCEs is their capability to analyze the stability of generic trajectories of nonlinear, non-autonomous dynamical systems. For this purpose, Hammond's ground resonance model is modified using lead-lag dampers characterized by a nonlinear constitutive law, to verify the application of the method to nonlinear problems. The simple nonlinear constitutive law of the damper considered in Ref. [33] (a moment that is quadratic in the angular velocity, to model turbulent viscous flow, with saturation) is modified by adding a linear term to the quadratic characteristic, yielding the moment

$$f_d = \begin{cases} \chi\dot{\zeta}|\dot{\zeta}| + C_L\dot{\zeta} & |\dot{\zeta}| < \dot{\zeta}_L \\ \bar{\chi}\mathrm{sign}(\dot{\zeta})\dot{\zeta}_L^2 & |\dot{\zeta}| \geq \dot{\zeta}_L \end{cases} \tag{39}$$

about the lead-lag hinge, where $\chi = \bar{\chi} - C_L/\dot{\zeta}_L$ to ensure that the value of damping at the discontinuity points $|\dot{\zeta}| = \dot{\zeta}_L$ remains the same when the slope at zero angular velocity, C_L, is changed. The slope is chosen as the parameter for investigating the sensitivity of the LCE estimates. It is expressed as a fraction of the nominal linear damper C_d given in Ref. [29]. The same values of Ref. [33] are used for the other parameters, as reported in Table 1.

In the model of Ref. [33] the slope C_L is zero, and Limit Cycle Oscillations (LCO) are observed. Without the linear term, the model is not realistic, since flow in a hydraulic damper tends to be laminar at small flow rates. Thus, the linear term better describes the physics of the device in the low angular rate $\dot{\zeta}$ regime.

Indeed, this problem has been selected to obtain a LCO in an otherwise reasonably realistic model and to test estimation of LCEs and their sensitivity with a nonlinear, non-autonomous problem that may include LCO, exponential stability, and unstable equilibria.

The blade lag motion ζ (only one of four blades is shown for clarity) is discussed first. Figure 3 shows the blade lag motion when the blade experiences LCO ($C_L = 0$) and exponential stability ($C_L = C_d$). In both plots, simulations start from different initial conditions. In Fig. 3a, the curves tend to oscillations with the same amplitude and period, thus confirming the limit cycle interpretation of the attractor. It is worth noticing that the trivial solution $\zeta = 0$ is also an equilibrium solution; however, since solutions obtained with initial conditions close to $\zeta = 0$ converge to the LCO rather than vanishing, $\zeta = 0$ is topologically an unstable equilibrium point. The present analysis for $\zeta = 0$ as the fiducial trajectory estimates a positive largest LCE, thus confirming its instability when $C_L = 0$. On the contrary, Fig. 3b shows that when $C_L = C_d$, the resulting curves converge to $\zeta = 0$, confirming that such fiducial trajectory is now a stable point.

If the system has a periodic attractor, a so-called LCO, zero-valued LCE estimates (or values very close to zero in a numerical sense) are expected [34]. In order to observe this and also further investigate sensitivity, LCEs and their sensitivity are estimated for a range of damper slopes at zero lag rate, C_L. Results are shown in Fig. 4a for LCEs and in Fig. 4b for sensitivity of LCEs. Although all LCE estimates have been computed, only the largest ones are shown for clarity, since they are the most critical with respect to stability. In the latter Figure, the analytical sensitivity is compared with the corresponding values obtained using finite differences: $\lambda_{i/p}|_{p_j} = (\lambda_i|_{p_{j+1}} - \lambda_i|_{p_{j-1}})/(p_{j+1} - p_{j-1})$. As one can observe from Fig. 4a, starting from $C_L = 0$ the largest LCE is zero and remains approximately zero until $C_L \approx 0.35C_d$. Hence, a LCO occurs in this range after the system encounters a perturbation. For larger values of C_L, the two largest LCEs (nearly) merge (i.e. they become numerically quite close to each other) and the system becomes exponentially stable with all LCEs negative. The differences in Fig. 4b between sensitivities computed using finite differences and the proposed approach can be explained by considering that both approaches contain approximations. Finite differences computed from LCE estimates suffer from truncation in LCE estimation and approximation in the finite differentiation process; estimated LCE sensitivity suffers from truncation in LCE estimation. The differences are maximal in proximity of large gradients in the sensitivity.

The previously discussed behavior is verified by looking at the lag motion of the blade. In Fig. 3a, which corresponds to $C_L = 0$, the blade motion converges to a stable LCO with magnitude 0.015 deg. Increasing the zero lag rate slope provides asymptotic stability: for example, when $C_L = C_d$, all LCEs are negative; Fig. 3b shows an exponentially stable motion. The sensitivity analysis of Fig. 4b can successfully capture this trend of stability properties.

The time evolution of LCE estimates corresponding to the cases of Fig. 3 is shown in Fig. 5. In the case resulting in an LCO, ($C_L = 0$, Fig. 3a and Fig. 5a), the two largest LCE estimates are distinct. The largest LCE, λ_1, quickly converges to zero, corresponding to the stable LCO with magnitude 0.015 deg. A

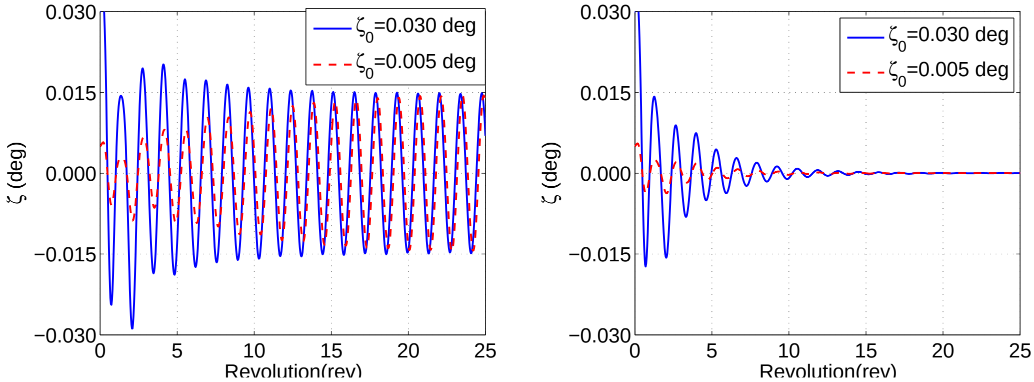

(a) LCO ($C_L = 0$) (b) Exponentially stable ($C_L = C_d$)

Figure 3: Helicopter ground resonance with nonlinear blade damper: blade lag motion starting from different initial conditions.

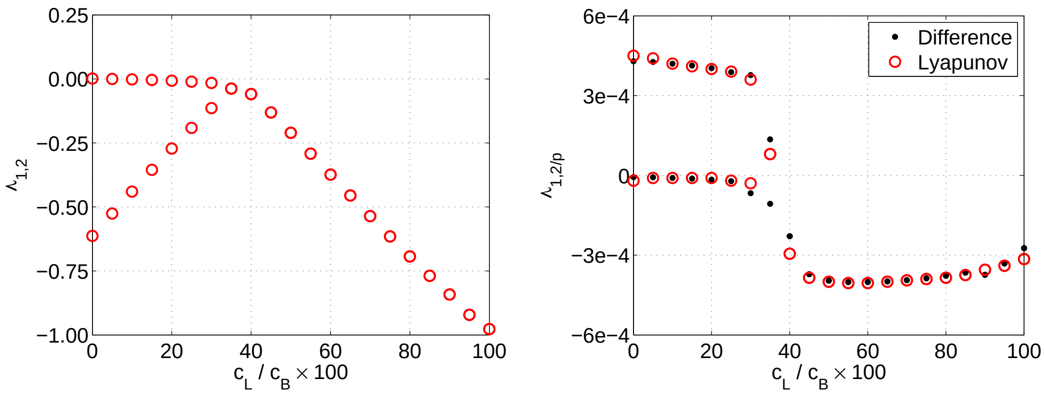

(a) Largest LCEs (b) Sensitivity of largest LCEs

Figure 4: Helicopter ground resonance with nonlinear blade damper: two largest LCE estimates and their sensitivity with respect to damper slope at zero lag rate C_L.

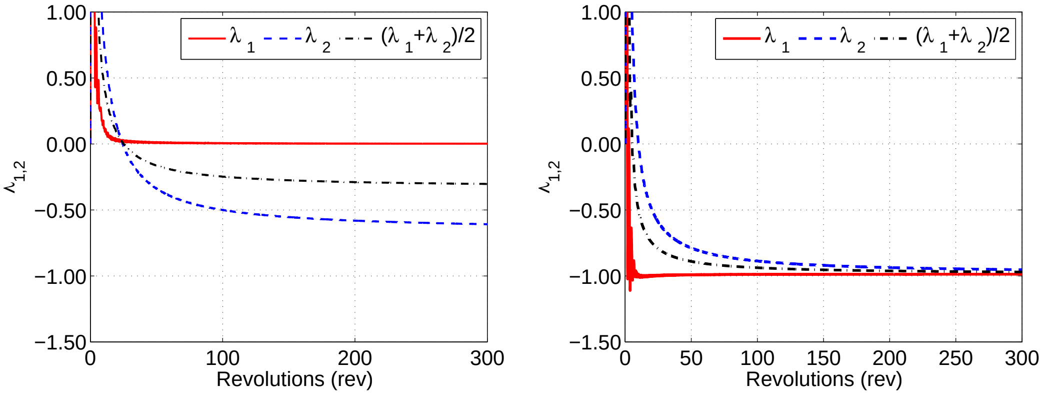

(a) LCO ($C_L = 0$) (b) Exponentially stable ($C_L = C_d$)

Figure 5: Helicopter ground resonance with nonlinear blade damper: time evolution of largest two LCE estimates.

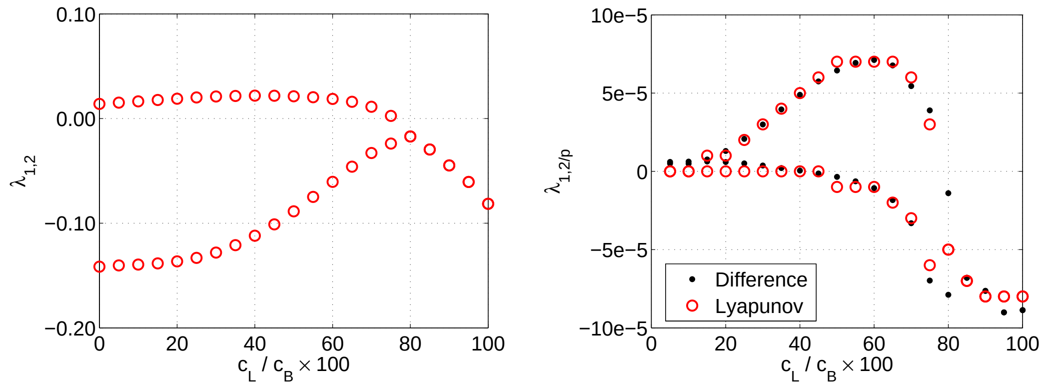

(a) Largest LCEs (b) Sensitivity of largest LCEs

Figure 6: Helicopter ground resonance with dissimilar nonlinear blade damper: two largest LCE estimates and their sensitivity with respect to damper slope at zero lag rate C_L.

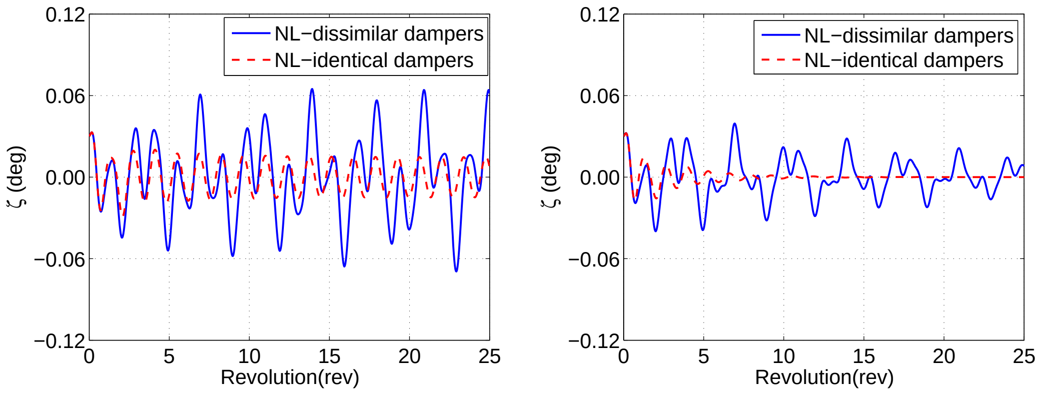

(a) Chaotic ($C_L = 0$)

(b) Exponentially stable ($C_L = C_d$)

Figure 7: Helicopter ground resonance with dissimilar nonlinear blade damper: blade lag motion starting from different initial conditions, compared with the isotropic rotor case.

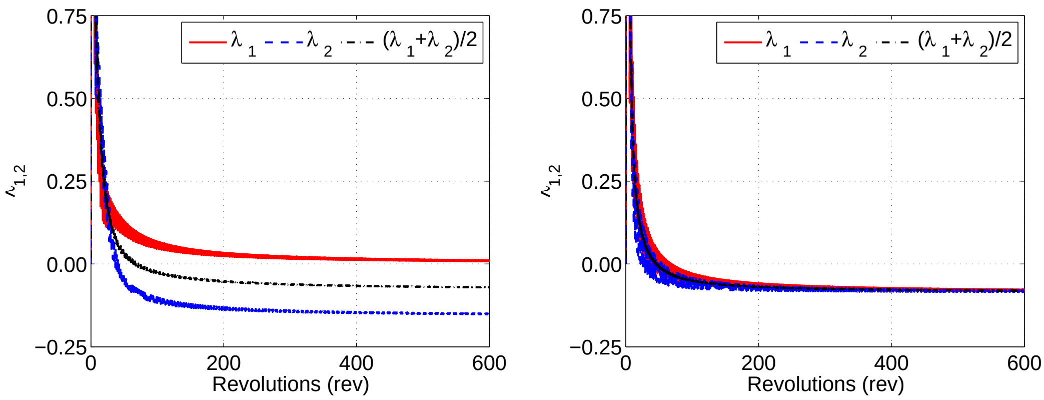

(a) Chaotic ($C_L = 0$)

(b) Exponentially stable ($C_L = C_d$)

Figure 8: Helicopter ground resonance with dissimilar nonlinear blade damper: time evolution of two largest LCE estimates.

zero-valued LCE indicates an LCO; hence, the LCE estimates and the time simulations are in agreement. Increasing the slope at zero lag rate provides stability; for a sufficiently large value of C_L (for example Fig. 3b and 5b), the two largest LCE estimates converge to the same value, suggesting that they are coincident, with multiplicity 2, as if they were associated with complex conjugated eigenvalues in a LTI system. This solution is stable, as observed from the time simulations and indicated by the negative largest LCEs.

3.3. Helicopter Ground Resonance with Dissimilar Nonlinear Lead-Lag Dampers

In order to apply the proposed approach to a nonlinear non-autonomous problem, one damper is removed from the model considered in the previous ground resonance example with nonlinear dampers; thus the symmetry is spoiled and time dependence is introduced. The linear damping characteristic (C_L) of the nonlinear damping force is again used as parameter. Stability and sensitivity analyses are performed for the same parameter range. The two largest LCEs are shown in Fig. 6a as functions of the percentage of linear damping C_L. In the C_L/C_d region up to 75% the largest LCE is greater than zero. Since, as described in Ref. [34], for a nonlinear system with a bounded trajectory a positive LCE indicates chaos, this region is expected to experience a somewhat chaotic motion. For damping greater than 75% of the nominal value the largest two LCEs become negative; thus, a stable behavior is expected.

Fig. 6b presents the analytical sensitivity results of the largest two LCEs, compared with corresponding results obtained by applying finite differences to LCE estimates of Fig. 6a. While the slope of the positive LCE remains almost zero for C_L/C_d up to 40% and then slowly decreases until a C_L/C_d of about 75%, that of the other one is initially positive until a C_L/C_d of about 75%, then it decreases abruptly, and the two LCEs merge and take the same negative slope. Analytical and finite difference results are reasonably close and follow a similar pattern.

In order to verify the LCE indications, we can further analyze the two extreme points of Fig. 6a. Fig. 7a shows the lag motion of one blade (only one blade is presented for simplicity) when the remaining dampers have null slope at zero lag rate ($C_L = 0$), compared with the curve of Fig. 3a, namely the corresponding results of an isotropic rotor with identical nonlinear dampers. The solution is not converging to an equilibrium point or a periodic orbit, but at the same time it remains within a bounded region of the state space. In fact, this is a distinctive property of chaos: a never repeating bounded trajectory, as explained in [32, 34]. Hence, the positive largest LCE and the chaotic motion of the blade are in agreement. The time evolution of LCEs for this case is given in Fig. 8a, which shows two separate LCEs.

Fig. 7b presents the lag motion of the blade for the remaining dampers having nominal slope at zero lag rate ($C_L = C_d$). Again there is no dominant period and the motion seems arbitrary, but this time the amplitude converges to zero, indicating that the solution is stable. The corresponding evolution of the LCE estimates is presented in Fig. 8b, showing two LCEs that converge to the same value, suggesting an LCE with multiplicity 2.

4. Conclusions

The sensitivity analysis of Lyapunov Characteristic Exponents with respect to system parameters is presented. Especially for several aerospace related applications, it is believed that time dependence, often in conjunction with non-strict periodicity and quasi-periodicity, as well as nonlinearity, cannot be neglected. Lyapunov Exponents correspond to the real part of the eigenvalues of the state matrix for linear time invariant systems, and to Floquet multipliers for linear time periodic systems; hence, they represent a natural generalization of stability indicators that are familiar in current engineering practice. Therefore, analytical sensitivity analysis of Lyapunov Exponents formulated in this work can proficiently support the sensitivity analysis of systems with an increasing level of complexity. The method is illustrated in relation with linear time periodic, nonlinear time invariant and nonlinear non-autonomous problems. Lyapunov Exponents estimations that have been shown to be compatible with Floquet-Lyapunov analysis and time marching simulations are analyzed for sensitivity. The results of Lyapunov Exponents analytical sensitivity are compared with corresponding ones obtained with Floquet-Lyapunov's theory for linear time periodic problems and with results obtained using centered finite differences for nonlinear problems. An acceptable level of agreement has been found in all cases, especially far from strong gradients.

It is noted that multiplicity of LCEs can be inferred by considering nearly periodic oscillations in LCE estimates that tend to very close values. After de-trending, the period in the oscillations of Lyapunov Exponents average can be associated with the period of linear time periodic problems. When correctly recognized as Lyapunov Exponents with higher multiplicity, the average of their estimate presents a much faster convergence to the correct value. The latter aspects need further investigation to improve the robustness of such considerations.

5. Acknowledgments

This research was not sponsored, nor received any funding.

References

[1] L. Perko, Differential Equations and Dynamical Systems, 3rd Edition, Texts in Applied Mathematics, Springer, New York, 2001.

[2] A. J. Roberts, The application of centre-manifold theory to the evolution of system which vary slowly in space, The Journal of the Australian Mathematical Society. Series B. Applied Mathematics 29 (04) (1988) 480–500, doi:10.1017/S0334270000005968.

[3] L. Y. Adrianova, Introduction to Linear Systems of Differential Equations, Vol. 146 of Translations of Mathematical Monographs, American Mathematical Society, Providence, Rhode Island, 1995.

[4] G. Benettin, L. Galgani, A. Giorgilli, J.-M. Strelcyn, Lyapunov characteristic exponents for smooth dynamical systems and for Hamiltonian systems; a method for computing all of them. part 1: Theory, Meccanica 15 (1) (1980) 9–20, doi:10.1007/BF02128236.

[5] N. D. Cong, H. Nam, Lyapunov's inequality for linear differential algebraic equation, Acta Mathematica Vietnamica 28 (1) (2003) 73–88.

[6] N. D. Cong, H. Nam, Lyapunov regularity of linear differential algebraic equations of index 1, Acta Mathematica Vietnamica 29 (1) (2004) 1–21.

[7] V. H. Linh, V. Mehrmann, Lyapunov, Bohl and Sacker-Sell spectral intervals for differential-algebraic equations, J. Dyn. Diff. Equat. 21 (2009) 153–194, doi:10.1007/s10884-009-9128-7.

[8] V. H. Linh, V. Mehrmann, Approximation of spectral intervals and leading directions for differential-algebraic equation via smooth singular value decompositions, SIAM Journal on Numerical Analysis 49 (5) (2011) 1810–1835, doi:10.1137/100806059.

[9] V. Linh, V. Mehrmann, E. Van Vleck, QR methods and error analysis for computing Lyapunov and Sacker-Sell spectral intervals for linear differential-algebraic equations, Advances in Computational Mathematics 35 (2–4) (2011) 281–322, doi:10.1007/s10444-010-9156-1.

[10] P. Masarati, Estimation of Lyapunov exponents from multibody dynamics in differential-algebraic form, Proc. IMechE Part K: J. Multi-body Dynamics 227 (4) (2013) 23–33, doi:10.1177/1464419312455754.

[11] S. Rao, Engineering Optimization: Theory and Practice, 3rd Edition, John Wiley & Sons, 1996.

[12] B. Krauskopf, H. M. Osinga, J. Galán-Vioque, Numerical continuation methods for dynamical systems, Springer, 2007.

[13] A. Tamer, P. Masarati, Linearized structural dynamics model for the sensitivity analysis of helicopter rotor blades, in: Ankara International Aerospace Conference, Ankara, TR, 2013.

[14] G. Orosz, G. Stépán, Hopf bifurcation calculations in delayed systems with translational symmetry, Journal of Nonlinear Science 14 (6) (2004) 505–528, doi:10.1007/s00332-004-0625-4.

[15] I.-C. Shih, A. M. Spence, R. Celi, Semianalytical sensitivity of Floquet characteristic exponents with application to rotary-wing aeroelasticity, Journal of Aircraft 33 (2) (1996) 322–330, doi:10.2514/3.46941.

[16] L. Dieci, E. S. Van Vleck, Lyapunov and other spectra: a survey, in: D. Estep, S. Taverner (Eds.), Collected lectures on the preservation of stability under discretization, SIAM, Philadelphia, PA (USA), 2002, Ch. 11, pp. 197–218.

[17] L. Dieci, E. S. Van Vleck, Lyapunov and Sacker-Sell spectral intervals, Journal of Dynamics and Differential Equations 19 (2) (2007) 265–293, doi:10.1007/s10884-006-9030-5.

[18] K. Geist, U. Parlitz, W. Lauterborn, Comparison of different methods for computing Lyapunov exponents, Progress of Theoretical Physics 83 (5) (1990) 875–893, doi:10.1143/PTP.83.875.

[19] L. Dieci, E. S. V. Vleck, On the error in computing Lyapunov exponents by QR methods, Numerische Mathematik 101 (4) (2005) 619–642, doi:10.1007/s00211-005-0644-z.

[20] L. Dieci, E. Van Vleck, Perturbation theory for approximation of Lyapunov exponents by QR methods, Journal of Dynamics and Differential Equations 18 (3) (2006) 815–840, doi:10.1007/s10884-006-9024-3.

[21] L. Dieci, C. Elia, The singular value decomposition to approximate spectra of dynamical systems. theoretical aspects, Journal of Differential Equations 230 (2) (2006) 502–531, doi:10.1016/j.jde.2006.08.007.

[22] L. Dieci, C. Elia, SVD algorithms to approximate spectra of dynamical systems, Mathematics and Computers in Simulation 79 (4) (2008) 1235–1254, doi:10.1016/j.matcom.2008.03.005.

[23] L. Dieci, E. S. Van Vleck, Lyapunov spectral intervals: Theory and computation, SIAM Journal on Numerical Analysis 40 (2) (2002) 516–542, doi:10.1137/S0036142901392304.

[24] C. S. Hsu, On approximating a general linear periodic system, Journal of Mathematical Analysis and Applications 45 (1) (1974) 234–251.

[25] D. A. Peters, S. M. Lieb, L. A. Ahaus, Interpretation of Floquet eigenvalues and eigenvectors for periodic systems, Journal of the American Helicopter Society 56 (3) (2011) 1–11, doi:10.4050/JAHS.56.032001.

[26] A. Tamer, P. Masarati, Periodic stability and sensitivity analysis of rotating machinery, in: Proceedings of the 9th

International Conference on Rotor Dynamics IFToMM ICORD 2014, Milan, Italy, 2014.

[27] G. D. Padfield, Helicopter Flight Dynamics: The Theory and Application of Flying Qualities and Simulation Modelling, AIAA Education Series, 1996.

[28] R. P. Coleman, A. M. Feingold, Theory of self-excited mechanical oscillations of helicopter rotors with hinged blades, Report 1351, NACA (1958).

[29] C. E. Hammond, An application of Floquet theory to prediction of mechanical instability, Journal of the American Helicopter Society 19 (4) (1974) 14–23, doi:10.4050/JAHS.19.14.

[30] G. Bir, Multiblade coordinate transformation and its application to wind turbine analysis, in: ASME Wind Energy Symposium, Reno, Nevada, 2008, NREL/CP-500-42553.

[31] R. L. Bielawa, Rotary Wing Structural Dynamics and Aeroelasticity, 2nd Edition, AIAA, Washington, DC, 2005.

[32] S. H. Strogatz, Nonlinear Dynamics and Chaos: With Applications to Physics, Biology, Chemistry, and Engineering, Perseus Books, Reading, Massachusetts, 1994.

[33] G. Quaranta, V. Muscarello, P. Masarati, Lead-lag damper robustness analysis for helicopter ground resonance, J. of Guidance, Control, and Dynamics 36 (4) (2013) 1150–1161, doi:10.2514/1.57188.

[34] A. Medio, M. Lines, Nonlinear Dynamics — A Primer, Cambridge University Press, 2001.